Laser and Particle Beams (1986), *vol.* 4, *part* 2, *pp.* 193–213
Printed in Northern Ireland

Magnetic self-compression in laboratory plasmas, quasars and radio galaxies. Part I

By ERIC J. LERNER
20 Pine Knoll Drive, Lawrenceville, NJ 08648

(Received 2 July 1985: revised 15 October 1985)

A model of quasars and their associated jets as phenomena of magnetic self-compression is presented. Magnetic field self-compression, as observed in laboratory plasma focus devices, results in increases in energy density of more than 10^8 and in even larger increases in transferred power density. Our model, based on the scaling of these phenomena to astrophysical dimensions, avoids the problems of gravitationally-confined approaches. It presents a mechanism by which the energy of a quasar is immediately derived from a volume nearly 10^6 times larger than the observed quasar radiating volume and is ultimately derived from the volume of an entire protogalactic plasma cloud. The model's predictions of quasar energy, radiated power, lifetime, dimensions, density and rotational velocity are in good agreement with observations. Part II of this paper extends the model to radio galaxies and briefly discusses the role of similar self-compression processes in the origin of filamentary super-clusters of galaxies.

1. Introduction

Quasars are characterized by extremely high energy and power densities. A powerful quasar may have a radiated power density (power/unit volume) 10^{16} to 10^{18} times greater than that of a large galaxy. What accounts for this high energy and power density? Most existing theories (for example, Abramowicz & Piran 1980; Lynden-Bell 1978) view this as a result of the gravitational self-compression of a large object to form either a black hole or a rapidly spinning, gravitationally-confined spinar. In contrast to this gravitationally confined approach, electromagnetic models conducive to laboratory astrophysical investigation have been proposed (Sturrock 1969; Alfven 1978; Peratt & Green 1983; Browne 1985). The importance of magnetic fields in confining cosmic jets (Benford 1978; Chan & Henrikson 1980; Potash & Wardle 1980) and in their production (for example, Belvedere & Molteni 1982) has been discussed by many researchers. Laboratory experiments using the plasma focus device suggest that magnetic field interactions could also account for the concentration of energy in the quasar itself.

The present proposed model, like other electromagnetic quasar models, hypothesizes an electromagnetically confined concentration of energy in the quasar. Like Browne (1985) we see magnetic field self compression or pinching as the primary process in the production of high energy and power densities. Our model, however, goes beyond those proposals in that we develop here a specific mechanism for compression and derive specific quantitative predictions.

Increases of energy density of 10^8 over initial values have been repeatedly observed in the plasma focus, with the energy being concentrated in self-contained plasma lumps (plasmoids) with sharply defined boundaries. When the internal currents in such plasmoids suddenly decay (as in the opening of a switch with vanishingly small

0263-0346/86/0402–0193$05.00

inductance), the magnetic energy is converted in a nanosecond time interval to particle energy in two oppositely directed collimated beams of high-energy electrons and ions. During the decay of the plasmoid structure, emitted power densities within the decaying plasmoids are well in excess of 10^9 times the inflowing power density of the initial currents in the focus device (Nardi 1974).

In the present paper we assume that the observed phenomenon of magnetic self-compression of laboratory plasmas also occurs on an astrophysical scale in the origin of quasars and their accompanying jets. This phenomenon explains how the energy in large-scale intergalactic fields such as those observed around active galaxies can, in the course of galaxy formation, be concentrated into much smaller volumes and then released in intense collimated beams or jets.

The model we develop shows how the energy reservoir for the quasar is contained in a much larger volume of space than that of the observed quasar itself, and thus the difficulties encountered by gravitationally-contained models are avoided.

In § 2 the laboratory observations of magnetic self-compression and its theoretical explanation are summarized. In § 3 the quasar model is presented. § 4 is a quantitative comparison of the model and observations. In Part II the model is extended to radio galaxies and the production of intergalactic magnetic fields by self-compression is discussed.

2. Magnetic self-compression in the plasma focus

Magnetic self-compression is observed in the plasma focus, a device used in the generation of relativistic electron beams and controlled thermonuclear reaction research. The focus, proposed by Filippov and Mather (Filippov *et al.* 1961; Mather 1965a; 1965b), is extremely simple in structure, consisting of two concentric cylindrical electrodes, across which a capacitor bank, or other energy storage device, is rapidly discharged. Many authors (e.g. Bernard 1978; Bertalot 1981; Bostick *et al.* 1974; Cebanu *et al.* 1981; Ivanov *et al.* 1981; Nardi 1974; Yokoyama *et al.* 1981) have described in detail the sequence of events occurring in the plasma between the electrodes that lead to magnetic field self-compression (figure 1).

Initially, a current sheath forms in the plasma between the electrodes. This current sheath is propelled down the coaxial electrodes by the interaction of the radial currents with the azimuthal component of the B-field produced by the electrode currents.

Experimental results and theoretical work indicate that the streaming of the plasma against the B-field generates vortex filaments. These are force-free, self-pinched structures with J parallel to B, helical current flow, and helical mass plasma flow, (figure 2), (Bostick *et al.* 1966; Nardi 1970; 1974).

The filaments are formed in contrarotating pairs, with the B-fields and mass flows alternatively parallel and anti-parallel. These filaments are typically half a millimeter to a millimeter in diameter. Their longitudinal B-fields allow the sheath to carry a current far in excess of the Alfven limit ($17\,000\,\beta\gamma$) (Yoshikawa, 1971).

When the current sheath reaches the end of the electrodes, the filamentary current sheath converges on the electrode central axis, forming a hollow column along this axis. The column self-pinches, necking off into a number of toroidal vortices or plasmoids (figure 3). In this process, pairs of vortex filaments merge and annihilate each other through rapid reconnection of magnetic field lines, inducing currents along the axial sheath, with peak J in the axial region, far in excess of the peak J of the electrodes.

The result of this process is the compression of a large fraction of the entire energy

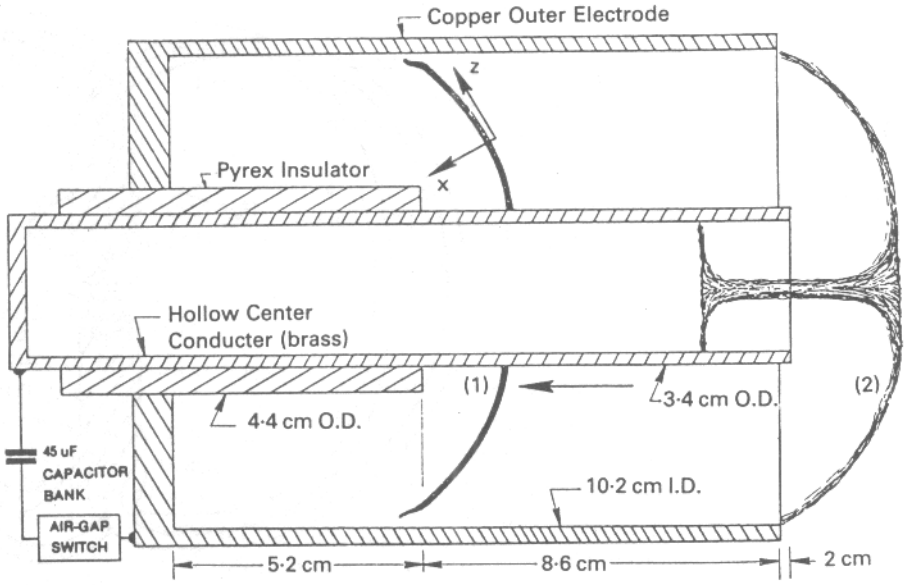

FIGURE 1. Cross section of typical plasma-focus device. Plasma sheath is shown while moving down electrodes and at time when plasmoids are produced.

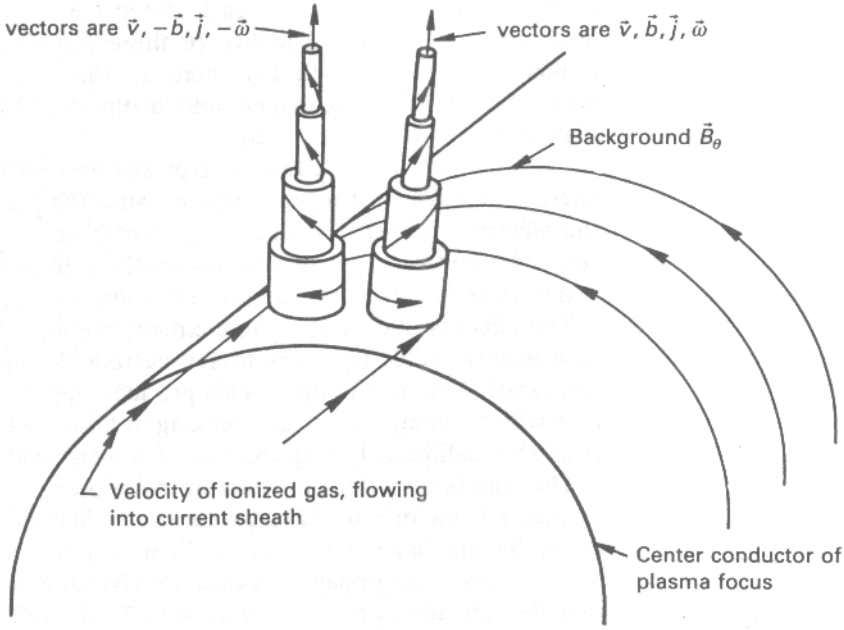

FIGURE 2. Structure of paired vortex filaments; v is mass flow velocity, b is local magnetic field, j is current density, ω is vorticity and B is background field. Note that filaments allow plasma to flow through field while keeping the angle between local field and mass flow small. Also note that pitch of magnetic field in filaments decreases towards the central axis of the filaments.

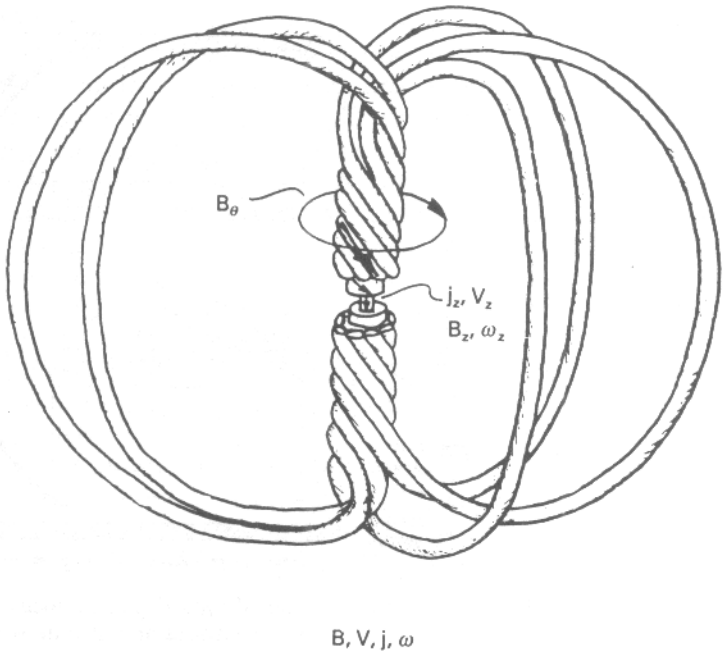

FIGURE 3. As filaments converge towards electrode, pinch is formed. Out of necked-off plasma channel, plasmoid, made up of vortex filaments, and shown here schematically, is formed.

stored in the magnetic field of the initial radial currents into the volume of the plasmoids. Since initially the magnetic field is contained in the inter-electrode volume of the device (typical radius 5 cm), and at the end of this self-compression the magnetic field energy is contained in two or three plasmoids (each with a central axial region radius 50 microns, length 400 microns), the overall increase in energy density of the field is about 10^8. Peak magnetic fields up to 200 MG are produced on the axis of the plasmoids (Bostick *et al.* 1975).

During most of their lifetime (typically around 100 nsec), the plasmoids do not lose energy from synchrotron radiation because the plasma within the plasmoids is opaque, the electron plasma frequency (ω_{pe}) being above the electron synchrotron frequency (ω_{ce}). However, as the plasmoids continue to self-pinch and the B-field in the axial region increases, the plasma becomes transparent, allowing a rapid radiation of energy.

The effect is that of opening a circuit; the inductive field dB/dt generates extremely high electric fields to maintain the current despite the huge rise in (non-collisional) resistance. The accelerating fields produce oppositely-directed beams of electrons and ions with an energy spectrum peaking at about 300–400 kev (when the applied voltage is 15 kV), collimated along the axis of the electrodes (within a 6° cone) (Nardi 1983).

The emerging electron beam is composed typically of 10^3 filaments ranging in diameter from one to 300 microns. Each filament is formed of many smaller fibers (typically one micron or less in diameter) which can maintain their structure over several meters of propagation distance (Nardi *et al.* 1980). Experimental tests indicate that the fine structure of the emerging beams reflects the filamentary structure of the decaying plasmoids that produce the beams.

Observations of ion clumps with particle densities 10^{22} to 10^{23} cm^3 and diameters of 1 to 100 microns within the outgoing ion beam filaments indicate that the beam production mechanism is not a smooth, continuous process, confirmed also by Hayd *et*

al., (1984). The composite beam pulses are produced by the disruption of individual micro-filaments (Nardi 1983). This is confirmed by observations that the electron beam is broken up into pulses of picosecond length (Herziger 1983).

In typical experiments, the power transferred to the beam per unit volume of the plasmoids as a whole is at least 2×10^{16} W/cm^2, nearly 10^9 the power/unit volume initially transferred into the device. The power per unit volume in individual micro-filaments is six orders of magnitude greater still.

3. A model for quasars

Our model of quasars is based on a process of magnetic self-compression similar to that occurring in the plasma focus. The initial conditions are those of a contracting, rotating, protogalactic cloud of gas in an intergalactic magnetic field with a component parallel to the axis of rotation. The existence of intergalactic magnetic fields in clusters of galaxies has been observed (Vrotonyi 1980). We will show in Part II why such fields are to be expected. The model requires only that there is a component of the magnetic field parallel to the axis of rotation, since other components, in the case of a rotating body, can be neglected, since they have no net effect over the course of a rotation, in agreement with previous analyses (Parker 1981).

As in the plasma focus, the situation involves plasma streaming against perpendicular lines of magnetic force. The dynamical situations are different in that in the quasar model the plasma motion is azimuthal and the field axial, while in the focus the motion is axial and the field azimuthal. However, on the scale of the filaments the large-scale differences are not significant in that, locally, the plasma motion and magnetic field are orthogonal (figure 4). (Similarly, the absence of the coaxial electrodes in the astrophysical case is not physically significant. The role of the inner electrode in creating the plasma focus in the laboratory is simply to redirect the radial currents towards the axial direction, causing them to converge. This same redirection occurs naturally in the astrophysical case as the radial current bends around to move outward along the axis of rotation.) Radial vortex filaments will be generated, paired contra-rotating and co-rotating (B field and velocity vectors anti-parallel or parallel), above and below the plane of rotation. These filaments allow the plasma in the rotating protogalaxy to move through the perpendicular background field with a minimum of energy loss, since at all points the angle between the local stream flow and local magnetic field will be small.

The net slippage of the plasma through the lines of the background field generates a radial E-field acting along the helical filaments. On the largest scale, the contracting protogalaxy acts as a plasma disk generator producing currents that flow towards the center in the plane of rotation where the plasma density is highest and away from the center along the axis of rotation, as has been analyzed by Alfven (Alfven 1981). On the scale of the filaments the E-field and currents are helical, lying parallel to the magnetic and fluid flow lines in the filaments. The filaments are, thus, as in the plasma focus, force-free.

Initially, the current flow is symmetric, with half the current flowing out along the axis in the direction of the rotation vector, the other half flowing out in the opposite direction. (But, at a later time, this symmetry will be broken.)

By this point in the process, the self pinching of the filaments has already considerably concentrated the magnetic field energy, and the magnetic self-compression process now produces far more energy concentration than does the continuing gravitational contraction.

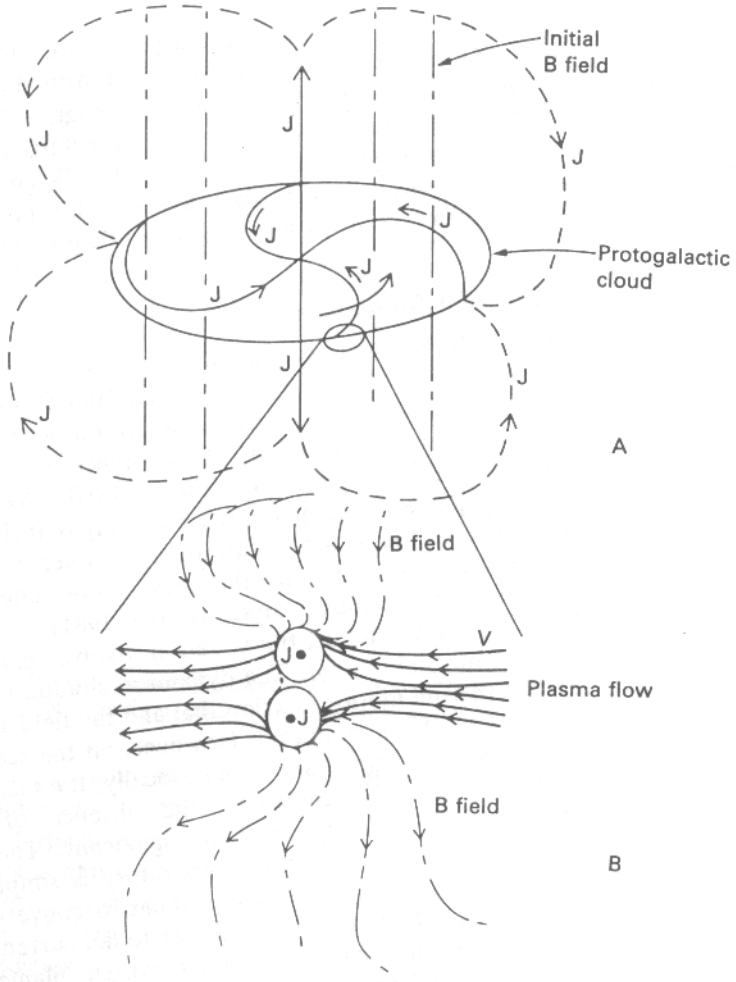

FIGURE 4. Rotation of contracting protogalactic cloud in external magnetic field (A) creates currents that flow radially inwards in plane of rotation, outwards along axis, connecting up at large distance from galaxy. (See Alfven 1981.) Vortex filaments (B) are created that carry current. In vicinity of filaments, B-fields and plasma flows are approximately parallel or anti-parallel. Within filaments B, j and v are all colinear, with top filament corotating and bottom contrarotating.

It may be objected that no significant slippage of plasma past field lines is possible on a cosmic scale, because the magnetic Reynolds number is exceedingly high. However, we are here dealing with a turbulent plasma, and the diffusivity term that is important here is not the molecular diffusivity, but the turbulent diffusivity, $\lambda V/L$ (where λ is the characteristic length of the largest turbulence cells, V the plasma flow velocity and L the characteristic length of the magnetic field cells) as has been pointed out by Parker (1981) and others in the general case of turbulent plasma. (We use the term turbulence here to mean any non-laminar flow, not necessarily random mass motions, since the vortices are themselves highly coherent, non-random phenomena.) As we shall show in the next section, when the turbulent diffusivity is considered, the effective magnetic Reynolds number is much lower than for a nonturbulent plasma, and, the magnetic Reynolds numbers can be treated as scale invariant. Since, as we shall demonstrate,

the effective magnetic Reynolds number is only of order unity, significant slippage of the plasma past the field lines is to be expected.

The equivalence of the situation to that of the plasma focus is clear, but the energy sources are different. In the focus, the energy source is an energy storage device, while in the quasar model the source of the energy is the rotation of the protogalaxy which generates the current.

The same sequence of events as in the plasma focus now occurs in the quasar model, by the same process of self-pinching leading to the formation of toroidal plasmoids containing all or most of the energy originally present in the magnetic field of the initial induced currents. As in the focus, when the B-field in the most central region of plasmoid exceeds B_{crit}, synchrotron radiation is radiated and axial emfs are generated, creating the two axial beams, electrons in one direction and protons in the other.

Once this generation of beams occurs in the most concentrated region of either the 'North' or 'South' branch of the current structure (figure 5), the initial symmetry of the structure is broken. The large current beams directed out of the decaying plasmoid create large-scale magnetic fields which will direct incoming currents into the branch from which the beams originated, disrupting the alternate branch. Just as in the focus, the beams are produced by the disruption of individual filaments, each much smaller than the plasmoid itself, and each producing a short pulse of ions and electrons. So, in the quasar model there is at any one instant a small central region within the plasmoid (energetically connected to the plasmoid as a whole) which is producing the observed beam and radiation pulses. This much smaller region within the plasmoid is what is observed as the quasar.

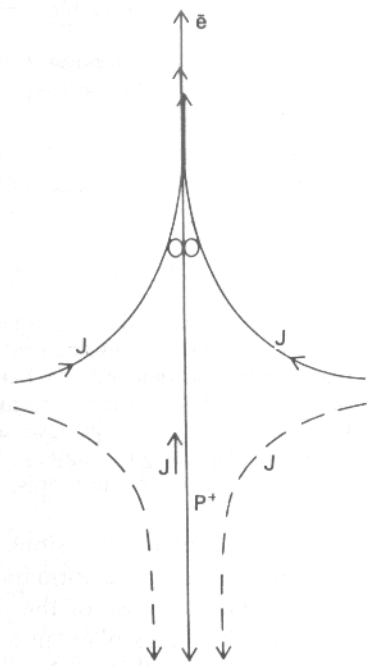

FIGURE 5. Initial inward currents run along the axis of rotation in both parallel and antiparallel directions, relative to the rotation vector. Once galactic plasmoid is formed on either side and begins emitting powerful electron and proton beams in opposite directions, current in proton beam sets up large magnetic field which disrupts opposing current pattern (dashed lines), thus channeling all currents into one branch.

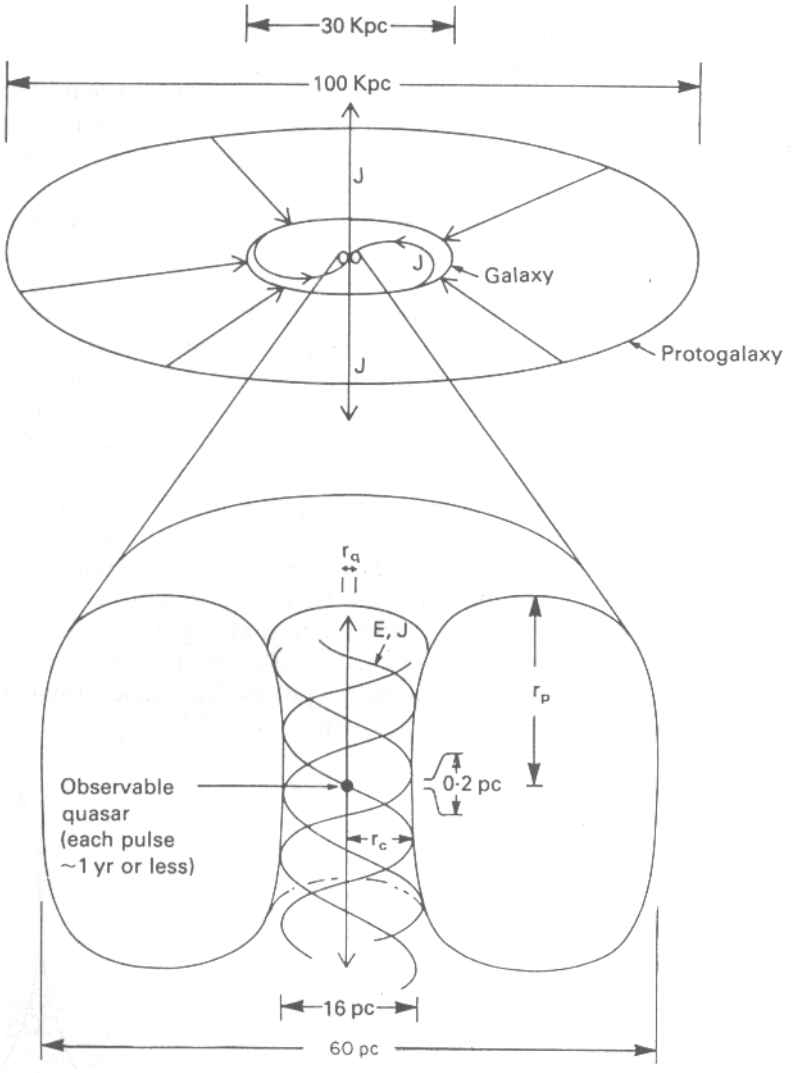

FIGURE 6. Quasar model involves two stages: stage I, creation of plasmoid, lasting some 10^8 years takes place during contraction of protogalaxy, leads to compression of large fraction of initial magnetic field energy being compressed within 30 pc radius plasmoid with 8 pc radius central core. Stage II is the decay of the plasmoid and the release of the stored magnetic energy to the beams. This stage lasts about 3×10^5 years. At any given time, transfer of energy is occurring with single filament, located at peak B field of plasmoid. This region of energy transfer, 0·2 pc or less in radius, is the quasar, emitting beam pulses lasting one year or less.

Thus, our model envisions two stages of energy and power compression (figure 6). The first stage is the formation of the plasmoid by magnetic compression during the gravitational collapse of the protogalaxy. As we will see in the following quantitative analysis, this takes place in a period of some few hundred million years (as compared with an analogous phase lasting around 1 microsecond in the plasma focus) and results in the generation of magnetic field energy in a volume with a radius of some tens of thousands of parsecs and the compression of this energy into a plasmoid with a radius of tens of parsecs. The second stage is the decay of the plasmoid, lasting some few hundred thousand years (as compared with an interval of the order of one nanosecond

in the plasma focus) when this energy is released. Here the total *power* being released by the galactic plasmoid as a whole is transferred to the beam in pulses lasting only a year or less and originating in a volume a fraction of a parsec in radius. The observed quasar (the small central volume) is thus drawing energy by magnetic induction from the much larger surrounding volume of the galactic plasmoid. While each quasar pulse lasts only a year or less, the quasar exists as a sequence of such pulses for the entire several hundred-thousand-year period of plasmoid decay.

Although gravitation plays a role in this model in the initial compression of the protogalaxy, the plasmoid is magnetically-, not gravitationally-confined.

4. Quantitative Analysis

We begin our quantitative analysis by proposing, on the basis of laboratory experiments and theoretical logic, a number of scale invariants, that is, quantities which do not change in going from the laboratory to the astrophysical scale. Second we use the laboratory observations to determine what the values of these invariants are (in some cases such values are also theoretically derived). Third, we propose some quantities that are constants of the motion during any given compression process. We then use these invariants and the constants of the motion to derive quantitative predictions from the model and finally, we compare these predictions with observations of quasars.

First of all, each phase of the self-compression of the magnetic field is characterized by a particular value of the $\omega_{ce}/\omega_{pe} \equiv Q$. For the decaying plasmoid, it is clear why Q is important: the plasmoid begins to decay when the plasma becomes transparent to electron synchrotron radiation, that is when $Q = 1$.

In the case of the initial conditions, we are seeking a parameter that characterizes the maximum instability of the plasma for production of force-free filaments, while for the filaments themselves we are seeking a parameter that defines the conditions of their stability against further self-pinching. Extensive previous analysis of plasma instabilities, and in particular the formation of filaments from ion and electron beams (for example, Buneman *et al.* 1966; Molvig 1975), show that the key governing parameter is Q.

Molvig's and other results show that where $Q < 1$, electron filamentation develops rapidly with a growth rate ω_{pe}, due to self-pinching of the electron current. Since the vorticity of the plasma plus that of the magnetic field is conserved, (see, for example, Ferraro & Plumpton 1961) for a plasma initially at rest, the electron filaments will develop a vorticity $\omega = -(e/m)B = \omega_{ce}$ where m is the electron mass.

This vorticity must, in some way, be transferred to the ions if mass vorticity of the plasma is to develop. It is only to the extent that electromagnetic energy is transferred from the current to the mass motion of the plasma that allows the anomalous resistance to develop, thus in turn allowing the maintenance of high E fields even when the ohmic resistance is low. We follow Bykovskii & Lagoda (1982) in hypothesizing that when the electron drift velocity V_d exceeds the speed of sound C_s in the plasma, electron currents can develop instabilities that generate ion acoustic oscillations, in effect, a form of shock wave. Under appropriate conditions, outlined below, these oscillations in both the current and the plasma can grow rapidly, generating mass flow of the plasma in the direction of the azimuthal current flow of the electrons, and thus transferring the vorticity to the plasma. (In the following we assume, as do Bykovskii and Mikhailovskii (Mikhailovskii 1974) that the plasma is non-collisional, that is that the collisional relaxation times are much greater than the instability growth times. In fact, as we will

show in the Appendix of this paper, for all physically important situations, the mean free path is greater than or equal to the radius of the filaments.)

The first condition for this process occurring is that $V_d > C_s$. As Bykovskii and Lagoda demonstrated, the vortex filaments that form are composed of smaller microfilaments which have radii equal to

$$r_f'' = V_t\left(\frac{M}{m}\right)^{\frac{1}{2}} mc/eB' \tag{1}$$

where V_t is the electron thermal velocity, and B' is the average axial field, $B' = \frac{1}{2}B = I/r_f''c$, see Yoshikawa (1971), m is electron mass, M is proton mass. When the electron filaments reach equilibrium, the magnetic energy is equal to the kinetic energy of the electrons, so that

$$V_t = B/(4\pi nm)^{\frac{1}{2}} = (\omega_{ce}/\omega_{pe})c = Qc. \tag{2}$$

We then have, from (1) and (2) for each micro filament,

$$r_f'' = (M/m)^{\frac{1}{2}} Qmc^2/eB'. \tag{3}$$

Since $B' = I/r_f''c$, we get from (3)

$$I = Q(M/m)^{\frac{1}{2}} mc^3/e \tag{4}$$

(in statamperes). (I is the net current in the axial direction along the microfilament.) Now, $V_d = I/\pi n r_f''^2 e$. Since $Q = B/(4\pi nm)^{\frac{1}{2}}c = 2I/r_f''^2 c(4\pi nm)^{\frac{1}{2}}$, $Q^2 = I^2/r^2\pi c^4 nm = V_d Ie/mc^4$ and thus

$$V_d = Q^2 mc^4/Ie. \tag{5}$$

From (4) and (5), we get

$$V_d = (m/M)^{\frac{1}{2}} Qc = C_s. \tag{6}$$

So that, within the microfilaments, the drift velocity is just the sound speed of the plasma (although the drift velocity is much lower if averaged over the whole current-carrying area).

Given that initially the ions are cold, and thus $T_e \gg T_i$, we can expect the current to produce ion plasma oscillations, which, with $V_d = C_s$ will have a frequency of just ω_{pi}, the ion plasma frequency, see Mikhailovskii (1974). For such a Cherenkov instability, the maximal growth rate occurs at a frequency equal to ω_{ce}. This maximal growth rate is $3^{\frac{1}{2}}2^{-\frac{4}{3}}(m/M)^{\frac{1}{3}}\omega_{ce}$, which is fast compared with any other relevant times. The ion plasma oscillations generate mass flow in the direction of the axial current along the microfilaments. Since the microfilaments flow in the helical pattern of the overall force free filaments, this transfers the overall vorticity to the plasma mass motion. Thus the optimal conditions for vortex formations are when $\omega_{ce} = \omega_{pi}$.

It therefore seems reasonable to hypothesize that (for the initial conditions), when $\omega_{ce} = \omega_{pi}$, mass flow plasma vortices will form. Since $Q = \omega_{ce}/\omega_{pe}$, when $\omega_{ce} = \omega_{pi}$, $Q = (m/M)^{\frac{1}{2}}$.

We will return to the case of the incoming and outgoing filaments below.

We note that since Q is proportional to $B/n^{\frac{1}{2}}$ and thus to the Alfven velocity, there is also a characteristic Alfven velocity for each phase of the compression.

Second, the magnetic Reynolds number $R_m = V/V_D$, where V_D is the magnetic diffusivity velocity, should also be scale invariant. Since $V_D = \lambda V/L$ (Parker 1981), $R_m = L/\lambda$. Since in the vortex filaments we are considering, the ratio between these two lengths must be a constant of order unity, because the magnetic field and fluid

motions are everywhere colinear, R_m also must be an invariant and of order unity, at least for the filaments.

Since the energy in the filamentary structure is roughly equipartioned between magnetic field and kinetic energy, (which must be true if the magnetic compression and centrifugal forces are balanced) $V = V_A$, the Alfven velocity. Since V_A and R_m are scale invariant for each phase of the compression, so is V_D, and since the effective resistance $R = \mu_0 V_D$, the resistance is also a scale invariant for each phase.

The actual resistance can be directly calculated, at least roughly because it is entirely due to the transfer of kinetic energy to the plasma within the vortex. The power transferred to the plasma mass motion from the vortex current is $P = 10^7 I^2 R$. The kinetic energy of the vortex filament is $\frac{1}{2} M_f V_a^2$, where M_f is the mass of the filament. Now $M_f = \pi r_f^2 L n M$, where r_f is the filament radius and L is its length. The power needed to transfer this energy to a filament that is growing in length with velocity V_a is then just $(\pi r/2) r_f^2 V_a^3 n M$,. But $V_a = B/(4\pi n M)^{\frac{1}{2}} = I/5 r_f (4\pi n M)^{\frac{1}{2}}$. So we have, equating the power flowing from the current to that flowing to the plasma mass flow:

$$10^7 I^2 R = I^2 V_a / 200.$$

Thus $R = V_a/2 \times 10^9$, for the filament system. For the outgoing, relativistic beam, the filament grows in length at about c, so that $R_b = c/2 \times 10^9$ or roughly 15 ohms.

From these scale invariants, two scaling laws can be derived for the duration of various phases of the modeled compression. (For these and following calculations, currents are in amps, voltages in volts and resistance in ohms, while all other units are cgs.) The field energy present when the radial currents have peaked can be calculated as $B^2 r_f^2 r_i / 8$, where r_f is the filament radius and r_i is the radius of the whole plasma (and thus the length of the radial filaments). Since $B^2 = I^2/25 r_f^2$, the field energy is simply $I^2 r_i / 200$ ergs. The power of the current is $10^7 I^2 R$ erg/sec, where R is the effective resistance, V/I, where V is potential, and therefore the time it takes to establish the field energy, and thus the characteristic time t_1 of the initial phase of the compression is $r_i/2 \times 10^9 R$ sec/cm, or $(t_1 R/r_i) = 5 \times 10^{-10}$ sec/cm, another scale invariant.

Second, we consider the duration of the plasmoid decay, t_2, thus the lifetime of the quasar. We emphasize that the energy contained in the emitting volume of the quasar is radiated in a time much shorter than the lifetime of the quasar. It is the energy of the much larger plasmoid surrounding the observable quasar that determines the total life of the quasar.

Treating the plasmoid as a simple solenoid, we find that as the plasmoid loses energy over a characteristic time t_2, an electric potential is induced along the axis, $E = 10^{-2} \mu_0 \pi r_{pd} I_{pd} / t_2$ where I_{pd} is the plasmoid current and r_{pd} the plasmoid radius. If the effective resistance of the beam (defined as e_b/I_b where e_b is the particle energy in ev and I_b is the output beam current) is R_b, and each beam is accelerated from the center to the edge of the plasmoid by a potential $E/2$, then the total power of both beams together is $10^7 E^2/2R_b$ erg/s. Since over time t_2 the entire energy of the plasmoid is lost this energy is $10^7 E^2 t_2 / 2R_b$ erg. However, since the magnetic field energy in the plasmoid core region (length equal to $2r_{pd}$) is the total energy of the plasmoid before its decay and is equal to $I_{pd}^2 r_{pd}/100$ erg, we have

$$I_{pd}^2 r_{pd}/100 = 10^7 E^2 t_2 / 2R_b = 10^3 \mu_0^2 \pi^2 I_{pd}^2 r_{pd}^2 / 2 t_2 R_b \tag{7}$$

or

$$t_2 R_b / r_{pd} = \frac{10^5 \pi^2 \mu_0^2}{2} = 8 \times 10^{-9} \pi^4 \text{ ohm-sec/cm}. \tag{8}$$

Since $I_b = 10^{-2}\mu_0 \pi r_{pd} I_{pd}/2t_2 R_b$, where I_b is the current of each output beam, we get from (8) $I_b/I_{pd} = 1/10^7 \mu_0 \pi = 1/4\pi^2$. Assuming that the total B field at the axis is about $2\frac{1}{2} B_{avg}$ for the core of the plasmoid, the beam radius r_b is $(1/4\sqrt{2}\pi^2) r_c$, where r_c is the radius of the axial region.

Over times $\geq r_{pd}/c$, the output of the beam is determined by dI_{pd}/dt. Over times $< r_{pd}/c$, however, local fluctuations in the output beam caused by magnetic field reconnections on scales down to r_b are possible and in fact expected, leading bursts of beam current and more intense accelerating fields. In such fluctuations, local magnetic field energy lost through the production of the beam is replaced by induction from the rest of the plasmoid.

Such fluctuations can occur on scales larger than that at which the field energy in a region with radius r_f is exhausted by the beam in a time $t_f = r_f/c$, The minimum region that can produce such fluctuations is therefore defined by setting the energy of the beam generated in time $t_f = r_f/c$ equal to the field energy of the volume with radius r_f. Since the energy is proportional to the volume for approximately constant B, we have

$$\frac{\mathscr{E}_f}{\mathscr{E}_{pd}} = \mathscr{V}_f/\mathscr{V}_c = t_f/t_2 = r_f/ct_2 \tag{9}$$

Where $\mathscr{E}$ is magnetic energy content and $\mathscr{V}$ is volume. Laboratory observations show that $r_c/r_{pd} = 0{\cdot}25$ and thus the volume of the axial region is $8\pi r_c^3$ or $\pi r_{pd}^3/8$. For $\mathscr{V}_f$ defined as a cylinder of length r_f we have

$$\frac{\mathscr{V}_f}{\mathscr{V}_c} = 8r_f^3/r_{pd}^3 = r_f/ct_2 \tag{10}$$

or $8r_f^2/r_{pd}^2 = r_{pd}/ct_2$ and since $r_{pd}/t_2 = R_b/8 \times 10^{-9}\pi^4$, we have

$$r_f/r_{pd} = \frac{1}{8\pi^2}\left(\frac{R_b}{10^{-9}c}\right)^{\frac{1}{2}} \tag{11}$$

Since R_b is experimentally measured as 3.2 ohm (See table 1),

$$r_f/r_{pd} = 1/24\pi^2 \tag{12}$$

so that $r_f/r_b = 1$, that is, the minimum volume that can produce beam fluctuations comparable in power to the average beam output has roughly the same radius as the beam filament itself, as might be expected. It is this small volume at the center of the axial region that we take to correspond to the observable quasar.

There are some quantities that are not scale invariants but are approximate constants of the motion during a compression. One is the energy contained in the magnetic field as it undergoes compression. Second, once the filaments form, V the velocity vector of the plasma and the B vector are always colinear, so that the ratio B/n should be relatively constant during a compression. With this last relationship we can derive the

	I(amps)	V(volts)	Radius(cm)	$B(G)$	$n(\text{cm}^{-3})$
Initial Conditions	6×10^5	2×10^4	5	$2{\cdot}4 \times 10^4$	$1{\cdot}5 \times 10^{17}$
Incoming Filaments	4×10^4	2×10^4	$2{\cdot}5 \times 10^{-2}$	$3{\cdot}2 \times 10^5$	10^{18}
Decaying Plasmoid	$3 - 5 \times 10^6$	10^6	5×10^{-3}†	2×10^8	10^{21}
Outgoing Beams	$1{\cdot}25 \times 10^5$	4×10^5	5×10^{-2}	5×10^5	10^{18}

TABLE 1

† Core radius. Overall radius at time of maximum compression is about 2×10^{-2} cm.

approximate value of Q for the vortex filaments. The filaments will self-compress until ω_{cef} of the filament equals ω_{pep} of the background plasma (the cyclotron resonance condition). If ω_{cef} is more than ω_{pep}, energy can be transferred from the filament to the plasma, damping the vortex motion. $\omega_{cef} = \omega_{pep}$ is thus a stability condition for the filaments, or $B_f/n_p^{\frac{1}{2}} = 2\pi^{\frac{1}{2}} m^{\frac{1}{2}} c$. But $B_f/n_f = B_p/n_p$ and $Q_p = (m/M)^{\frac{1}{2}}$, therefore it can be calculated that $Q_f = (m/M)^{\frac{1}{4}}$.

Given this value of Q_f and the fact that $V_a = (m/M)^{\frac{1}{2}} Qc$ we have for the incoming filament system that the resistance $R = (m/M)^{\frac{1}{2}} Qc/2 \times 10^9 = (m/M)^{\frac{1}{4}} c/2 \times 10^9$ or about $\frac{1}{20}$ ohm.

We now turn to the laboratory observations to see if, in the lab, the relationships derived theoretically do hold, and so can be extrapolated to the cosmic scale, and what the values of the invariants not precisely determined theoretically are.

Table 1 presents a summary of actually observed quantities in laboratory experiments. The sources of the values presented in table 1 are found in Bostick *et al.* 1975; Nardi *et al.* 1978; Nardi *et al.* 1980; Nardi 1974; and Kitagawa *et al.* 1980. The initial conditions are those that maximize the beam outputs for a given energy input. Deuterium plasma is used throughout.

The results of Bostick, Nardi and co-workers are relied upon primarily because they provide a consistent set of figures on all phases of the plasma focus self-compression process. However, other researchers report similar values for initial conditions such as resistance and B^2/n (Jerzykiewicz 1983; 1984), for the radius of the axial region of the plasmoids (Haas 1983; Herziger 1983; and Schmidt 1983) and for the energy of the output beam (Hirano 1983). While other groups have not measured either density or magnetic field within the plasmoids, recent computer simulations (Imshennik 1984) have been consistent with the values of B^2/n Nardi and co-workers found in the plasmoids.

Table 2 shows quantities derived from the observed values. Table 3 summarizes the scale invariants. As predicted by the above analysis, the Q for the decaying plasmoid is unity if we take the peak B (observed) $= \sqrt{2}\, B_{avg}$ for the core (ω_{ce}/ω_{pe} is relativistically corrected $(m = m_0(1-\beta^2)^{\frac{1}{2}} = 2m_0)$ since the electrons are here accelerated to 400–500 kev). The ratio for the initial conditions is quite close to the anticipated figure of $(m/M)^{\frac{1}{2}} = 1{\cdot}65 \times 10^{-2}$, and for the filaments close to $(m/M)^{\frac{1}{4}} = 0{\cdot}13$.

R_m is of order unity for the filaments and the initial conditions, while B/n changes by only a factor of three, as expected with such a value of R_m and the colinearity of B and plasma mass flow. The energy content of the magnetic field is also constant, given that there are on average 2 to 3 plasmoids per plasma focus shot.

The observed R_i for the incoming filament system, 1/30 ohm is reasonably close to the calculated 1/20 ohm, although the observed beam resistance, $R_b = 3{\cdot}2$ ohm is considerably less than the roughly calculated 15 ohms, implying that the beam is composed of a number of smaller filaments, as is observed in the lab. Such smaller filaments will absorb less total kinetic energy, reducing the effective resistance.

	B/n	$B/n^{\frac{1}{2}}$	Gyro/ Plasma Frequency	Resistance (ohms)	Magnetic Reynolds	Energy (ergs)
Initial Conditions	$1{\cdot}6 \times 10^{-13}$	$6{\cdot}2 \times 10^{-5}$	2×10^{-2}	$3{\cdot}3 \times 10^{-2}$	3·6	9×10^9
Incoming Filaments	$3{\cdot}2 \times 10^{-13}$	$3{\cdot}2 \times 10^{-4}$	0·10	0·5	1·2	
Decaying Plasmoid	$2{\cdot}0 \times 10^{-13}$	$6{\cdot}3 \times 10^{-3}$	0·96	0·2	60	5×10^9
Outgoing Beams	$5{\cdot}0 \times 10^{-13}$	$5{\cdot}0 \times 10^{-4}$	0·16	3·2	0·3	5×10^9

TABLE 2

Quantity	Values	Derivation of values
1) $Q \equiv \omega_{ce}/\omega_{pe} \sim B/m^{\frac{1}{2}} \sim V_A$	Initial condition $Q_i = (m/M)^{\frac{1}{2}}$ Beam, Filament $Q_b = Q_f = (m/M)^{\frac{1}{4}}$ Plasmoid $Q_{pd} = 1$	$\omega_{ce} = \omega_{pi}$, by hypothesis from Q_i, B/n constant of motion, $\omega_{cef} = \omega_{pe}$ (plasma) At time of decay, transparent to cyclotron radiation, $\omega_{ce} = \omega_{ci}$
2) $R_m \equiv$ magnetic Reynolds number	$R_{mi} = 3{\cdot}6$ $R_{mf} = 1{\cdot}2$ $R_{mb} = 0{\cdot}3$ $R_{mpd} = 60$	Lab experiments
3) $V_A^2/V^2 \equiv$ magnetic/kinetic energy	1	From balance of magnetic and centrifugal forces
4) $R \equiv$ resistance $\sim Q/R_m$	$R_i = 3{\cdot}3 \times 10^{-2}$ ohm $R_f = 0{\cdot}5$ $R_b = 3{\cdot}2$ $R_{pd} = 0{\cdot}2$	From values of R_m, Q
5) $t_i R_i/r_i \equiv$ compression time/initial radius	5×10^{-10} sec ohm/cm	From EM theory
6) $t_2 R_b/r_{pd} \equiv$ decay time/plasmoid radius	8×10^{-7} sec ohm/cm	From EM theory
7) $I_b/I_{pd} \equiv$ beam/plasmoid current ratio = $r_b/r_{pd} \equiv$ beam/plasma radius ratio	$\frac{1}{4}\sqrt{2}\pi^2$	From EM theory
8) $r_c/r_{pd} \equiv$ radius of axial region/radius of plasmoid	0·25	Lab experiments

TABLE 3. Summary of scale invariants

Substituting the observed values for r_{pd} and R_b, and the observed value of 5 nsec for t_2, we find $t_2 R_b/r_p = 8 \times 10^{-7}$, as predicted, and $r_b/r_c = 1/50$, in close agreement with the predicted value of $\frac{1}{4}\sqrt{2}\,\pi^2$.

Using the laboratory results and invariant relations outlined above, we can now develop the model quantitatively and compare it with observations.

We first examine the induction of emf in a rotating, contracting protogalaxy in an external magnetic field and determine if the invariant relation for the initial conditions of the plasma-focus process is fulfilled, i.e., is $Q \approx 2 \times 10^{-2}$? This is equivalent to the ratio $B/n^{\frac{1}{2}} \approx 6 \times 10^{-5}\ Gcm^{\frac{3}{2}}$. (For a hydrogen plasma, the ideal initial conditions will be somewhat different, since in that case, $\omega_{ce} = \omega_{pi}$ when $B/n^{\frac{1}{2}} = 4 \times 10^{-5}\ Gcm^{\frac{3}{2}}$. If a value of $5 \times 10^{-5}\ Gcm^{\frac{3}{2}}$ is chosen, any errors introduced will be within the limits of accuracy of all observations.)

If we take the range of large galaxy masses to be 10^{11} to $10^{13}\,M$, and the range of initial cloud sizes to be 30–100 kpc radius (with the lower limit twice typical galactic radii and the upper limit based on typical spacings between galaxies), the range of densities in the cloud will be between $2{\cdot}5 \times 10^{-2}$ cc and 10^{-1} cc. With observed rotational velocities of the outer parts of galaxies ranging between 250 and 500 km/sec and the compression ratios (ratio of initial cloud radius to final galaxy radius) ranging from 2 to 6, initial rotational velocities will be typically $80 - 250$ km/sec, by conservation of angular momentum.

We can roughly calculate the induced emf by treating the rotating plasma cloud as a disk generator. While this is an approximation, it is accurate to a factor of two. At any given point in time, the actual emf will be increased over a solid disk approximation, because $d\Omega/dr \neq 0$ as it does in a solid disk. We deal with this by assuming $dv/dr = 0$, causing the emf to be doubled over that of the solid disk. This is still less than the velocity in the inner regions, but, on the other hand, for the actual emf, E_{act}, we can expect, $E_{act} < E_{calc}$ because the process will not be perfectly efficient. These corrections we estimate will approximately balance. Over the contraction time, the emf should not vary greatly on average, since it is proportional to vr, where v is velocity and r is radius of the plasma, and vr is a constant when angular momentum is conserved.

In cgs, we have emf, $E = 10^{-8} B_0 vr$, where B_0 is the background intergalactic magnetic field strength. The effective resistance we take as the same as in the plasma focus, 1/30 ohm, because as previously pointed out, resistance should be scale invariant. The induced current, therefore, is $3 \times 10^{-7} B_0 vr$ and the induced average magnetic field is $6 \times 10^{-8} B_0 v$. For initial rotational velocities of 80 to 250 km/sec, the induced field is 0·4 to $1{\cdot}25 B_0$.

For the condition of the plasma focus, $B'/n^{\frac{1}{2}} = 5 \times 10^{-5}$, to be fulfilled (where B' is the current self-field), the background intergalactic field must equal 0·4 to $1{\cdot}25 \times 10^{-4} n^{\frac{1}{2}}$. Since the higher initial velocities will occur together with the higher initial densities in the most massive clouds, this works out in all cases to an initial field of around 12 to 14 microG.

This field is quite reasonable by comparison with observed fields of similar extent in the vicinity of active galaxies. The field surrounding Virgo *A*, for example (Vrotonyi 1980), is estimated at 8 microgauss, with a radius of 50 kpc. It seems completely plausible that somewhat higher fields over somewhat larger regions commonly existed at the time most galaxies were forming. Therefore, we conclude that the initial conditions of protogalaxies prior to collapse do, at least in some cases, satisfy the invariant relations for plasma-focus compressions. In particular, we would expect to find such strong fields near the centers of large clusters.

We note that for initial velocities near 170 km/sec the induced field, B' (the self field

of the induced currents) is nearly equal to B_0, the external field. If the initial velocity of rotation of the protogalaxy, $v \ll 170$ km/sec then $B_0 \gg B'$. In this case filament formation would be inhibited, since the contribution of B_0 to the ratio $B/n^{\frac{1}{2}}$ would overwhelm that of B'. The dynamics would be dominated not by the interaction of the currents and the plasma, but by the initial field and the plasma.

Conversely, if $v \gg 170$ km/sec, the kinetic energy of the plasma would much exceed the magnetic energy, since for the conditions required for filament formation, V_A, the Alfven velocity is $(m/M)^{\frac{1}{2}}Qc$, which is $(m/M)c = 163$ km/sec when $Q = (m/M)^{\frac{1}{2}}$. In this case, filament formation would again be inhibited, since any incipient filaments would be continually disrupted by the much more energetic inherent motion of the plasma.

So that only for v of the order of 170 km/sec is filament formation possible. (However, once filaments are formed, their characteristic Alfven velocities are much higher, around 1000 km/sec, so they are not disrupted by increasing rotational velocities as the protogalactic cloud contracts.)

We next consider if the energy available in the magnetic field produced in the above manner is sufficient to power quasars.

It should be noted that in this initial situation, the Alfven velocities ($\sim mc/M$ or $\sim$170 km/sec) and fluid velocities are comparable and that the amount of energy eventually trapped in the magnetic field is comparable to the amount of rotational energy originally present. In the case of the smallest galactic clouds considered, this would be a substantial fraction of the final rotational energy, and therefore a substantial fraction of the total angular momentum will be transferred to the magnetic field. But in the case of the largest galaxies, only a few per cent of the final rotational energy will be in the magnetic field.

Since B'^2/n is a constant, the total energy of the magnetic field, and thus the total energy (E) available to the quasar, is proportional (because $E = B^2v/8\pi$ and $M_c = nvM$ and thus $E/M_c = B^2/8\pi nM$) to the mass of the cloud (M_c). For $B/n^{\frac{1}{2}} = 5 \times 10^{-5}$, $B^2/n = 2{\cdot}5 \times 10^{-9}$, $E/M_c = 6 \times 10^{13}$ erg/gm or $1{\cdot}2 \times 10^{47}$ erg/M_s, where M_s is the solar mass. For the range of masses considered, the range of energy is from $1{\cdot}2 \times 10^{58}$ ergs to $1{\cdot}2 \times 10^{60}$ ergs, in good agreement with the range of quasar energies actually observed.

For the range of conditions considered, the induced emf will be between 2×10^{17} and $1{\cdot}2 \times 10^{18}$ volts. Such enormous potentials can exist in the intergalactic plasma because the effective resistance of the plasma is high due to the turbulent diffusivity. The radial currents carried by all the filaments will be between 6×10^{18} and $3{\cdot}6 \times 10^{19}$ A.

From the scaling relationship for the compression phase duration derived above, we find the compression lasts $r_i/2 \times 10^9 R$ secs and since $R = 1/30$, this is $1{\cdot}5 \times 10^{-8} r_i$ or 50 to 150 million years, comparable with the time for gravitational contraction. The compression phase thus lasts approximately 3×10^{21} times longer in the quasar model than in the laboratory plasma focus, corresponding to the differences in linear dimensions.

We now turn to the details of the compression phase. We must take into account the influence of the simultaneous gravitational contraction of the plasma, which does not, of course, occur in the laboratory system. As the cloud contracts, the B/n ratio changes as matter slides down the lines of magnetic field towards the center. Since I is approximately constant during the contraction, the final B/n_f is therefore related to the initial B_i/n_i by $B_f/n_f = (r_i n_i / r_f n_f) B_i/n_i$.

We can now apply the invariant relations developed above to derive the parameters of the central plasmoid and quasar in terms of the compression ratios, r_i/r_f and n_f/n_i. We define $C \equiv r_i n_i / r_f n_f$. In what follows, the subscript c refers to the conditions in the plasmoid core at the time of its decay, while i refers to the initial conditions before

contraction, and f the conditions of the protogalaxy as a whole at the end of contraction.

From the values of $B/n^{\frac{1}{2}}$ at the start of the self-compression process and during plasmoid decay (see table 2) we have

$$B_c^2/n_c = \left(\frac{2M}{m}\right) B_i^2/n_i. \tag{13}$$

Since the magnetic compression itself does not change the ratio B/n, we have

$$B_c/n_c = B_f/n_f = C^{-1}B_i/n_i. \tag{14}$$

Therefore,

$$B_c/B_i = 2MC/m \tag{15}$$

$$n_c/n_i = 2MC^2/m. \tag{16}$$

Since the energy in the magnetic field is conserved,

$$I_c^2 r_c/25 = I_i^2 r_i/400. \tag{17}$$

Combining equations (15) and (17) above, and noting that B_c, the average field in the core is $I_c/(5\sqrt{2}c)$, we find

$$I_c/I_i = 2^{-5/6}(M/m)^{\frac{1}{3}}C^{\frac{1}{3}} = 6{\cdot}9C^{\frac{1}{3}} \tag{18}$$

$$r_c/r_i = 2^{-\frac{7}{3}}(m/M)^{\frac{2}{3}}C^{-\frac{2}{3}} = 1{\cdot}3 \times 10^{-3}C^{-\frac{2}{3}}. \tag{19}$$

Since the emitting region of plasmoid has a radius $r_q = r_c/4\sqrt{2}\pi^2$, then

$$r_{q/r_i} = \frac{2^{\frac{1}{6}}(m/M)^{\frac{2}{3}}C^{-\frac{2}{3}}}{32\pi^2} = 2{\cdot}4 \times 10^{-5}C^{-\frac{2}{3}}. \tag{20}$$

Given the equipartition condition (invariant condition 3 of table 3) and the Q_{pd} (relativistically corrected) we can find the velocity of gases in the plasmoid, $V = Q_{pd}c2^{\frac{1}{2}}(m/M)^{\frac{1}{2}} = 9{\cdot}9 \times 10^3$ km/sec.

From the relation for duration (6 in table 3) and the observed value for $R_b = 3{\cdot}2$ ohms, we have that the duration of the decay, or the lifetime of the quasar is

$$t_2 = \frac{8 \times 10^{-7} r_p}{3{\cdot}2} = \frac{32 \times 10^{-7} r_c}{3{\cdot}2} = 10^{-6} r_c. \tag{21}$$

The current of the output beams $I_b = I_c/4\pi^2 = 0{\cdot}18C^{\frac{1}{3}}I_i$, the beam voltage $V_b = 0{\cdot}58C^{\frac{1}{3}}I_i$ and the total output power in erg/sec for both beams together is $2 \times 10^7 I_b V_b = 2 \times 10^6 C^{\frac{1}{3}} I_i^2$.

The mass of the plasmoid core can be directly calculated from the ratio B^2/n and is equal to $10^{-51}E_m M_s$, where E_m is the energy of the quasar and the mass of the emitting region, or the visible quasar is about $10^{-56}E_m M_s$.

If we now take the range of compression ratios, initial proto-galaxy radii and initial currents cited above and substitute into the just-derived relations, we can derive predictions for quasar parameters which can be compared with the range of values actually observed.

Taking into account the fact that the protogalactic cloud compresses itself more in the axial direction than in the radial directions, for a radial compression of between 2 and 6 we assume an increase in density of between 16 around 1300, so we have a range of compression ratios, C, from between 8 and 220.

For the initial range of values mentioned above, we have the magnetic field in the quasar is 0·3 to 15 G, the density is 1×10^4 to $1{\cdot}5 \times 10^7$, in fairly good agreement with the observed range of 10^5 to 10^8 (for example, see Greenstein and Schmidt, 1964); the quasar radius is 0·07 to 0·2pc, in good agreement with observed light variation periods of the order of one year. The duration of the quasars is 3×10^5 to 10^6 years, again in good agreement with observed quasar jets of 100 to 300 kpc in length. The output power is 3×10^{44} to 1×10^{47} erg/sec, spanning the observed quasar powers.

The general range of quantitative parameters of the model, therefore, agrees quite well with those observed for actual quasars (table 4).

The model predicts quite well the observed constancy of gas velocities within quasars. The spectroscopically-determined maximum velocities within quasars cluster quite closely around the predicted value of 9900 km/sec (average observed $V =$ 9500 km/sec) (Baldwin & Netzer 1978). This is a phenomenon that is not easily derived from the black hole model.

The magnetic quasar model leads to much smaller masses for the quasars themselves than does the black hole model. The plasmoid core will have masses ranging from $2{\cdot}6 \times 10^7$ to $2{\cdot}6 \times 10^9 M_s$ while the region emitting the beams will be much smaller, about 10^2 to $10^4 M_s$.

The plasmoid currents will be $1{\cdot}4 \times 10^{20}$ to $2{\cdot}5 \times 10^{21}$ A and the output beam currents will be 0·4 to 1·2 times the input currents or $3{\cdot}10^{18}$ to 5×10^{19} A. The voltage of the beams is $1{\cdot}1 \times 10^{19}$ to 2×10^{20} V. As in the focus, the $B/n^{\frac{1}{2}}$ in the beams should be around 5×10^{-4}.

Not many jets from quasars have been observed, but a comparison can here be made with one of them, 4 *c* 32.69 (Potash & Wardle 1980). The jet has magnetic fields and radii that vary slowly along its length. Taking the values at the halfway point, the magnetic field is 62 microgauss and the radius 23 kpc, implying a current of 2×10^{19} A, comfortably within the range predicted. The length of the jet, 600 000 light-years, implies a 6×10^5 year lifetime, again within the range predicted. Given an overall energy content of 4×10^{59} ergs, the average power output is $2{\cdot}7 \times 10^{46}$ erg/sec and the voltage of the beam is therefore 7×10^{19} V, also within the range predicted. The ratio $B/n^{\frac{1}{2}}$ is observed as $5{\cdot}5 \times 10^{-4}$, close to the predicted value, and the effective resistance, 3·5 ohms, is also close to the 3·2 ohms expected.

Another confirmation of the predicted range of particle beam energies is in the

Quantity	Predicted value or range	Based on invariant	Observed
B_i initial field	12–14μG	Q_i	$>8\,\mu G$
energy	$1{\cdot}2 \times 10^{58} - 1{\cdot}2 \times 10^{60}$ erg	Q_i	$10^{57} - 10^{60}$ 2×10^{59}†
n_q density	$1 \times 10^4 - 1{\cdot}5 \times 10^7$/cc	Q_i, Q_p	$10^5 - 10^8$
r_q radius	0·07 – 0·2pc	Q_i, Q_p, r_b/r_c, r_c/r_p	0·01 – 1
t_2 lifetime	$3 \times 10^5 - 10^6$ years	$t_2 R_b/r_p$, R_b	$3 \times 10^5 - 10^6$, 6×10^5†
P_q power	$3 \times 10^{44} - 1 \times 10^{47}$ erg/s	I_b/I_p, R_b	$10^{43} - 10^{48}$ $2{\cdot}7 \times 10^{46}$†
V_q gas velocity	$9{\cdot}9 \times 10^3$ km/s	Q_p, V_a^2/V^2	$9{\cdot}5 \times 10^3$ km/s
I_b current	$3 \times 10^{18} - 5 \times 10^{19} V$	I_b/I_p, Q_i, Q_p	2×10^{19}†
V_b voltage	$1{\cdot}1 \times 10^{19} - 2 \times 10^{20} V$	I_b/I_p, Q_i, Q_p, R_b	7×10^{19}†
$B_b/n_b^{\frac{1}{2}}$	5×10^{-4}	Q_b	$5{\cdot}5 \times 10^{-4}$†
R_b effective resist.	3·2 ohms	R_b	3·5†

TABLE 4. Predicted and observed quantities

† Refers to 4c 32.69 (see text).

observed cosmic ray spectrum, which exhibits a broad peak in the range 10^{19} to -2×10^{20} ev, exactly corresponding to the range of particle energies anticipated.

Many researchers, including Benford, Potash & Wardle (Benford 1978; Potash & Wardle 1980), have pointed out that the well-ordered magnetic fields running parallel along quasar and active radio-nuclei jets can most easily be interpreted as helical currents which provided the confinement for the narrowly collimated jets. Again, the production of such powerful currents is difficult to account for in black hole models, but flows naturally out of the present model. Force-free current filaments account not only for the confinement of energy in the beam, but in the quasar as well.

Appendix

In our analysis of the formation of vortex filaments, we assumed that the filaments could be considered non collisional, that is that the time of formation of the microfilaments, of which the larger filaments are composed, is less than the collision time. Another condition is that the radius of the microfilaments is smaller than the mean free path.

We here examine what limitations this assumption places on our analysis.

The collision time, $T_c = \dfrac{M^2 v^3}{e^4 n 8\pi \ln \Lambda 0{\cdot}714}$, where $\ln \Lambda$ is the Coulomb logarithm. The mean free path, $D = vT_c$. The characteristic e-folding time T_g for the growth of the vortex filaments is $3^{-\frac{1}{2}}2^{\frac{4}{3}}(m/M)^{-\frac{1}{3}}\omega_{ce}^{-1}$ and the radius of the microfilaments equal to the ion gyroradius is mcv/eB.

Taking v as the Alfven velocity, $B/(4\pi nM)^{\frac{1}{2}}$ we have, when $T_c > T_g$,

$$\frac{B^3 M^{\frac{1}{2}}}{32\, 2^{\frac{1}{2}} 0{\cdot}714 \pi^{\frac{5}{2}} \ln \Lambda e^4 n^{\frac{5}{2}}} > \frac{m^{\frac{2}{3}} M^{\frac{1}{3}} c}{3^{\frac{1}{2}} 2^{-\frac{4}{3}} eB}$$

or,

$$\frac{3(B^2/n)^4 (M/m)^{\frac{1}{3}}}{2^{\frac{2}{3}} 2^{13} \pi^5 (0{\cdot}714)^2 (\ln \Lambda)^2 e^6 c^2 m} > n.$$

Since, we have found that for vortex formation, $\omega_{ce} = \omega_{pi}$ and therefore $B^2/n = 4\pi m^2 c^2/M$, we have $\dfrac{1}{32\pi} 2^{-\frac{2}{3}} (0{\cdot}714)^{-2} (\ln \Lambda)^{-2} r_e^{-3} (M/m^{-\frac{11}{3}}) = 6 \times 10^{23}/(\ln \Lambda)^2 > n$, where $r_e = e^2/mc^2$, the classical electron radius. So for all n less than about 2×10^{22}, the first condition holds, that is for all laboratory and all astrophysical situations, except within stars.

The second condition requires that $r_f < D$. For the filament, $v = (m/M)^{\frac{1}{4}} c$, so that

$$D = (m/M)/8\pi 0{\cdot}714 \ln \Lambda r_e^2 n = 3{\cdot}9 \times 10^{20}/n \ln \Lambda$$

$$r_f = (m/M)^{\frac{3}{4}} Mc^2/eB.$$

Since here $B^2/n = 4\pi (m/M)^{\frac{1}{2}} mc^2$, we have $\dfrac{1}{16\pi} (0{\cdot}714)^{-2} (\ln \Lambda)^{-2} r_e^{-3} (M/m)^{-3} = 2{\cdot}8 \times 10^{26}/(\ln \Lambda)^2 > n$, which is less restrictive than the first condition.

Acknowledgements:

The author wishes to thank Dr. Vitorio Nardi, Stevens Institute of Technology for his extremely extensive discussions, suggestions and criticism of this manuscript, and also Dr. Anthony Peratt of Los Alamos National Laboratory for his support and encouragement. I also thank Dr Winston Bostick, Stevens Institute of Technology, for his permission to use figures 1, 2 and 3, which were originally published by him.

REFERENCES

Abramowicz, M. A. & Piran, T. 1980 *Ap. J.* **141,** L7.

Alfven, H. 1978 *Astrophysics and Space Science,* **54,** 179.

Alfven, H. 1981 *Cosmic Plasma,* D. Reidel.

Baldwin, J. A. & Netzer, H. 1978 *Ap. J.*, **226,** 1.

Belvedere, G. & Molteni, D. 1982 *Ap. J.* **263,** 611.

Benford, G. 1978 *MNRAS,* **183,** 29.

Bernard, A. 1978 *Atomkernergie,* **32,** 73.

Bertalot, L. *et al.* 1981 *Proc. 8th IAEA Conf. on Plasma Physics and Controlled Nuclear Fusion,* 177.

Bostick, W. *et al.* 1966 *Phys. Fluids,* **9,** 2078.

Bostick, W. *et al.* 1974, *Proc. Int. Conf. on Energy, Storage, Compression and Switching,* 261.

Bostick, W. *et al.* 1975 *Ann. NY Acad. Sci.* **251,** 2.

Browne, P. F. 1985 *Ast. and Astrophys.* **144,** 298.

Buneman, O. *et al.* 1966 *J. Ap. Physics,* **37,** 3203.

Bykovskii, Y. A. & Lugoda, V. B. 1982 *JETP,* **56,** 61.

Cebanu, A. *et al.* 1981, *Proc. 8th IAEA Conf. on Plasma Physics and Controlled Nuclear Fusion,* 197.

Chan, K. L. & Henriksen, R. W. 1980 *Ap. J.* **241,** 534.

Ferraro, V. and Plumpton, C. 1961 *An Introduction to Magneto-Fluid Mechanics,* Oxford University Press.

Filippov, N. V. *et al.* 1961 *Proc. 1st IAEA Conf. on Plasma Physics and Controlled Nuclear Fusion,* 577.

Greenstein, T. L., & Schmidt, M. 1964 *Ap. J.* **140,** 1.

Haas, C. R. *et al.* 1983 *Proc. 3rd International Workshop on Plasma Focus Research,* 87.

Hayd, A., Kaeppeler, H. J., Maurer, M. & Meinke, P., 1984 *Proceed. Int. Conf. Plasma Physics, Lausanne, June,* Vol. 1, p. 166.

Herziger, G. *et al.* 1983 *ibid.* 31.

Hirano, K., *et al.* 1983 *ibid.* 35.

Imshennik, V. S. *et al.* 1984 *Proc. 10th IAEA Conf. on Plasma Physics and Controlled Nuclear Fusion,* 561.

Ivanov, V. D. *et al.* 1981 *Proc. 8th IAEA Conf. on Plasma Physics and Controlled Nuclear Fusion,* 161.

Jerzykiewicz, A. *et al.* 1983 *Proc. 3rd International Workshop on Plasma Focus Research,* 17.

Jerzkiewicz, A. *et al.* 1984 *Proc. 10th IAEA Conf. on Plasma Physics and Controlled Nuclear Fusion,* 591.

Kitagawa, Y. *et al.* 1980 *Proc. Int. Conf. Plasma Theory and 4th Int. Congress on Waves and Instabilities in Plasmas,* **1,** 164.

Leorat, J. *et al.* 1981 *J. Fluid Mech.* **104,** 419.

Lynden-Bell, D. 1978 *Phys. Scripta,* **17,** 185.

Marscher, A. P. & Broderick, J. J. 1981 *Ap. J.* **249,** 406.

Mather, J. W. 1965 (A), *Proc. 2nd IAEA Conf. on Plasma Physics and Controlled Nuclear Fusion,* **2,** 389.

Mather, J. W. 1965 (B) *Phys. Fluid.* **8,** 366.

Mikhailovskii, A. B. 1974 *Theory of Plasma Instabilities,* vol. 1, Consetants Bureau.

Molvig, K. 1975 *Phys. Rev. Let.* **35,** 1504.

Nardi, V. 1970 *Phys. Rev. Lett.* **25,** 778.

Nardi, V. 1974 *Proc. of Int. Conf. on Energy Storage, Compression and Switching,* 173.

Nardi, V, 1983 *Energy Storage, Compression and Switching II,* Plenum Press, p. 449.

Nardi, V. *et al.* 1978 *Proc. IAEA Conf. Plasma Phys. and Controlled Nuclear Fusion Research,* **2,** 143.

NARDI, V. *et al.* 1980 *Phys. Rev.* **224,** 2211.

PARKER, E. W. 1981 *Cosmical Magnetic Fields,* Oxford University Press.

PERATT, A. L. & Green, J. C. 1983 *Astrophysics and Space Science,* **91,** 19.

POTASH, R. J. & WARDEL, J. F. C. 1980 *Ap. J.* **239,** 42.

SCHMIDT, H. *et al.* 1983 *Proc. 3rd International Workshop on Plasma Focus Research,* 63.

STURROCK, P. A. 1969 in *Quasars and High-Energy Astronomy,* Gordon and Breach, New York, p. 167.

VROTONYI, K. 1980 *Ast. and Astrophys.* **83,** 245.

YOKOYAMA, M. *et al.* 1981 *Proc. 8th IAEA Conf. on Plasma Physics and Controlled Nuclear Fusion,* 187.

YOSHIKAWA, S. 1971 *Phys. Rev. Let.* **26,** 295.